Tritiated steel micro-particles: computational dosimetry and prediction of radiation-induced dna damage for in vitro cell culture exposures

Alice Mentana, Yordenca Lamartinière, Thierry Orsiere, Véronique Malard, Mickaël Payet, Danielle L Slomberg, Isabella Guardamagna, Leonardo Lonati, Cristian Grisolia, Awadhesh Jha, et al.

Tritiated Steel Micro-Particles: Computational Dosimetry and Prediction of Radiation-Induced DNA Damage for In Vitro Cell Culture Exposures

Authors: Mentana, Alice, Lamartinière, Yordenca, Orsière, Thierry, Malard, Véronique, Payet, Mickaël, et al.

Source: Radiation Research, 199(1) : 25-38

Published By: Radiation Research Society

URL: https://doi.org/10.1667/RADE-22-00043.1

RADIATION RESEARCH **199**, 25–38 (2023)
0033-7587/23 $15.00

DOI: 10.1667/RADE-22-00043.1

Tritiated Steel Micro-Particles: Computational Dosimetry and Prediction of Radiation-Induced DNA Damage for In Vitro Cell Culture Exposures

Alice Mentana,[a,1] Yordenca Lamartinière,[b] Thierry Orsière,[b] Véronique Malard,[c] Mickaël Payet,[d] Danielle Slomberg,[e] Isabella Guardamagna,[a] Leonardo Lonati,[a] Cristian Grisolia,[d] Awadhesh Jha,[f] Laurence Lebaron-Jacobs,[c] Jerome Rose,[e] Andrea Ottolenghi,[a] Giorgio Baiocco[a,1]

[a] Laboratory of Radiation Biophysics and Radiobiology, Department of Physics, University of Pavia, Pavia, Italy; [b] Aix Marseille Univ, Avignon Université, CNRS, IRD, IMBE, Marseille, France; [c] Aix Marseille Univ, CEA, CNRS, BIAM, Saint Paul-Lez-Durance, France; [d] CEA, IRFM, F-13108, Saint Paul-Lez-Durance, France; [e] Aix Marseille Univ, CNRS, IRD, INRAE, Coll France, CEREGE, Aix-en-Provence, France; [f] School of Biological and Marine Sciences, University of Plymouth, Plymouth, United Kingdom

Mentana A, Lamartinière Y, Orsière T, Malard V, Payet M, Slomberg D, Guardamagna I, Lonati L, Grisolia C, Jha A, Lebaron-Jacobs L, Rose J, Ottolenghi A, Baiocco G. Tritiated Steel Micro-Particles: Computational Dosimetry and Prediction of Radiation-Induced DNA Damage for In Vitro Cell Culture Exposures. Radiat Res. 199, 25–38 (2023).

Biological effects of radioactive particles can be experimentally investigated in vitro as a function of particle concentration, specific activity and exposure time. However, a careful dosimetric analysis is needed to elucidate the role of radiation emitted by radioactive products in inducing cyto- and geno-toxicity: the quantification of radiation dose is essential to eventually inform dose-risk correlations. This is even more fundamental when radioactive particles are short-range emitters and when they have a chemical speciation that might further concur to the heterogeneity of energy deposition at the cellular and sub-cellular level. To this aim, we need to use computational models. In this work, we made use of a Monte Carlo radiation transport code to perform a computational dosimetric reconstruction for in vitro exposure of cells to tritiated steel particles of micrometric size. Particles of this kind have been identified as worth of attention in nuclear power industry and research: tritium easily permeates in steel elements of nuclear reactor machinery, and mechanical operations on these elements (e.g., sawing) during decommissioning of old facilities can result in particle dispersion, leading to human exposure via inhalation. Considering the software replica of a representative in vitro setup to study the effect of such particles, we therefore modelled the radiation field due to the presence of particles in proximity of cells. We developed a computational approach to reconstruct the dose range to individual cell nuclei in contact with a particle, as well as the fraction of "hit" cells and the average dose for the whole cell population, as a function of particle concentration in the culture medium. The dosimetric analysis also provided the basis to make predictions on tritium-induced DNA damage: we estimated the dose-dependent expected yield of DNA double strand breaks due to tritiated steel particle radiation, as an indicator of their expected biological effectiveness. © 2023 by Radiation Research Society

[1] Corresponding authors: Alice Mentana, email: alice.mentana@unipv.it and Giorgio Baiocco, email: giorgio.baiocco@unipv.it. Laboratory of Radiation Biophysics and Radiobiology, Department of Physics, University of Pavia, Via Bassi 6, Pavia 27100, Italy.

INTRODUCTION

The dosimetric reconstruction at the cellular and sub-cellular level after radionuclide intake necessarily relies on computational tools. Dosimetric calculations are important to understand to what extent the spatial distribution of radioactive products, as well as their kinetics, affect the radiation dose distribution in a cell population. This is even more fundamental when dealing with short-range emitters, among which tritium is an extreme case: ^{3}H is a β-emitter, with a half-life of 12.3 years, and the average energy of emitted electrons is 5.7 keV, with a corresponding range in water/soft tissue of 0.5 μm. In most of the investigated scenarios of exposure to tritiated products, this very short range is compensated by a uniform distribution of sources: tritium is found mainly as tritiated water in the environment, either directly from natural sources (action of cosmic rays in the atmosphere) or from industrial activities in the nuclear power field and tritiated waste storage or treatments. Compared to other radionuclides, tritium is discharged in the environment in large quantities (*1*).

At present, due to deuterium-tritium fusion reactor development studies, as well as to the decommissioning of old nuclear power facilities, the tritium release in the environment is expected to increase, together with the related risk (*2*). Due to activities in the nuclear industry, tritium can be released into the atmosphere as tritium gas or tritiated water (*3*). When assimilated by living systems, organically bound tritium (OBT) compounds can be formed through biological processes. The radiotoxicological consequences of a contamination by tritiated water or

organically bound tritium have been identified during experiments in vitro, with cell culture models, or in vivo, with animal studies, mainly at high tritium concentrations (*3, 5*). Recently, also effects induced by low-dose tritium exposure have been investigated in vivo, with a large scale mice study (*6–9*) to examine both the biokinetics of tritium and the biological effects of chronic internal exposure, and in vitro in human mammary epithelial cells (*10*) and in human mesenchymal stem cells (*11*). Concerning human exposures, epidemiological studies have been conducted on workers, who have been exposed to tritium, but tritium-specific doses have hardly been the subject of a separate assessment (*12*). Taken all together, available studies do not provide at present a full assessment of the possible exposure levels and health risks posed by low-dose tritium exposure. Most importantly, previous studies have been limited to HTO and OBT as the most common tritiated products only (*4, 5*).

These considerations call for new studies addressing radiotoxicity, radiobiology and dosimetry for a wider range of tritiated products, as tritium is very mobile and can be absorbed in different materials. During the decommissioning of nuclear facilities, operations are intended to remove or eliminate any tritiated material. These operations generate fine airborne dusts, namely aerosols, with the possibility of having tritiated products with a particular chemical speciation, due to tritium interactions with building materials (*2*). In new fusion facilities, tritium also interacts with other elements, mainly beryllium and tungsten, leading to the formation of unique tritiated products. Tritiated stainless steel and cement particles have been recently identified as fusion/fission cross-cutting materials (*2*): these particles, expected to be produced with micro- and submicrometric size, might be dispersed in the environment and could lead to human exposure via e.g., inhalation. No previous studies exist on the possible impact of such tritiated products on the environment and human health.

Biological effects of tritiated steel and cement particles can be experimentally investigated in vitro as a function of particle concentration, specific activity and exposure time (*13, 14*). However, the chemical speciation and size of these products are such that a high heterogeneity of dose distribution is expected at the cellular and sub-cellular level. A careful dosimetric reconstruction with computational tools is therefore needed to properly interpret the outcome of experimental studies.

Within this context, the specific objective of our work was to perform a computational dosimetric reconstruction for in vitro exposure to tritiated steel micro-particles. We used the Monte Carlo radiation transport code PHITS (*15*) to build a software replica of a representative in vitro cell culture setup. Considering experimental information indicating that micrometric steel particles are not internalized by lung epithelial cells and, when tritiated, they release a fraction of their activity to the cell-culture medium (*13, 14*), we developed an approach to reconstruct the dose to individual cell nuclei in contact with a particle, the fraction of ''hit'' cells and the average dose for the whole cell population as a function of particle concentration in the culture medium. These calculations also aimed to provide indications on the expected biological damage induced to nuclear DNA by tritiated steel particles. We present here the strategy developed to achieve these objectives and the results obtained.

MATERIALS AND METHODS

Modelling a Representative Cell Culture Setup in Realistic Exposure Conditions

We developed a software model of an in vitro cell culture using as a reference the human bronchial epithelial cell line (BEAS-2B) cultured in adherent conditions as shown elsewhere (*13, 14*).

The simulations were performed using the Monte Carlo radiation transport code PHITS (version 3.22) (*15*) for the construction of the cell model, dosimetric assessment and characterization of the radiation field in cell nuclei. A database of results obtained with the biophysical code PARTRAC (*16*) was used to estimate biological effectiveness based on DNA damage induction by tritium β electrons.

In the literature (*13, 14*) the morphology of bronchial epithelial cells (BEAS-2B) treated with steel particles was studied acquiring confocal-microscopy images (*13*). We analyzed such confocal microscopy images with the software ImageJ (*17*), to extract geometrical information on BEAS-2B cells and build a representative software model. The top panel of Fig. 1 shows an example of a cell analyzed and reconstructed in 3 dimensions (3D). Average dimensions (obtained from ~50 cells) are presented in Table 1 (left column). For the in vitro measurements discussed previously (*13, 14*), commercially available SS316-L micrometric stainless-steel particles were used after a tritiation process. Such particles were found to have a fairly gaussian size distribution with average radius of 2.35 ± 0.68 μm (*18, 19*). In the computational model, we first assumed an average steel particle radius of $R = 2.35$ μm, as indicated in Table 1, and we then analyzed the impact of the particle size (as well as of an inhomogeneous distribution of particles and/or of the presence of particle aggregates) in the dosimetric results. The following parameters were chosen to describe the software cell geometry: r_n is the radius of the cell nucleus; l_1 and l_2 refer to the cytoplasm, whose shape is irregular and can vary from cell to cell; h is the cell thickness. Another important information extracted from microscopy images was the position of steel particles relative to cells. In particular, the image analysis led to the conclusion that steel particles are not internalized in lung epithelial cells (as it might be expected because of their size), but rather deposited on the cell surface, at different possible distances from cell nuclei. In some cases, some sort of ''depression'' in the cell membrane was observed, due to the weight of the particle. This possibly resulted in particles being closer to the nuclei, though not internalized. From the microscopy images it was however not possible to precisely estimate the thickness of the cytoplasm layer above the nucleus. For these reasons, a very thin cytoplasm layer (0.1 μm) above the nucleus was assumed and included in the software cell model, as detailed later. The dimensions extracted from the image analysis were combined with the information on the cell culture experimental conditions given in refs. (*13, 14*) (see Table 2) to build a software replica of a single cell in different realistic exposure conditions. In particular, as a representative case, we have considered the experimental conditions adopted to perform genotoxicity assay using the micronuclei assay (*13*), conducted on cells after exposure to tritiated particles for 24 h. Three different views of the software model are shown in Fig. 1 (bottom panels). The cell, whose cytoplasm (in

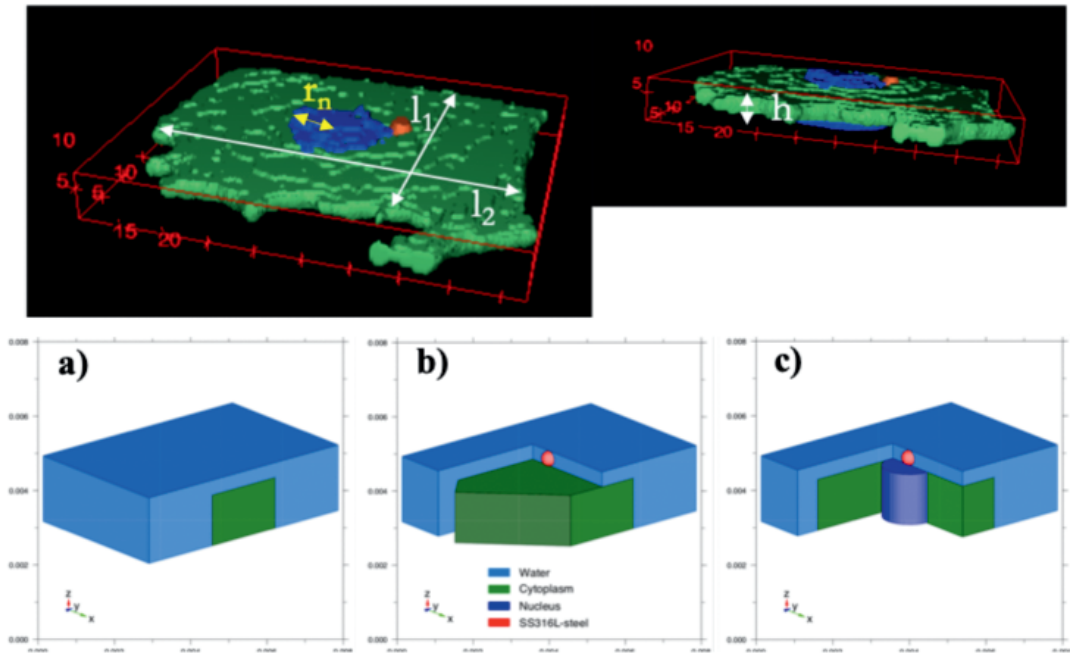

FIG. 1. Top panel: 3D reconstruction [FIJI software (*17*)] from confocal microscopy images of a bronchial epithelial (BEAS-2B) cell treated with steel particles (*13, 14*). Cell cytoplasm is colored in green, cell nucleus in blue and the particle deposited on the cell surface in orange. Bottom panel: the single-cell single-particle software cell model used for simulations (Monte Carlo transport code PHITS v.3.22). Panel a: Whole water volume unit (light blue) containing a single cell and a steel particle deposited on the surface. Panels b and c: Two cross-sectional views, highlighting the cell (central, cytoplasm in green) and the cell nucleus (right, in blue), with the steel particle (orange) in a central position.

TABLE 1
Information Used for the Software Model Reconstruction

Images and exp. characterization		Software model	
Cell		Cell	
r_n	8.00 μm	r_n	8.00 μm
l_1	47.00 μm	<l>	60.00 μm
l_2	49.00 μm	h_n	16.00 μm
h	16.00 μm	h_{cyto}	16.20 μm
		ρ_{cell}	1.06 g/cm^3
Steel particle		Steel particle	
R	2.35 μm ± 0.68 μm (*)	R	2.35 μm
		ρ_{steel}	7.75 g/cm^3
		Water volume	
		V_u	$7.22 \cdot 10^4$ μm^3

Notes. Left column: typical geometrical dimensions of BEAS-2B cells and radius of a steel particle (*Gaussian distribution with average value ± σ). r_n, l_1, l_2 and h refer to Fig. 1 (top panel) and are measured from confocal microscopy images. Images and experimental data are taken and used from the literature (*13, 14*) for a test of the computational approach for dosimetric reconstruction presented in this work. Right column: cell and steel particle dimensions and density used for the model (Fig. 1, bottom panel). Cell: r_n and h_n are the nuclear radius and height, <l> and h_{cyto} are the cytoplasm linear dimension and height, and ρ_{cell} is the water-like density of the cell. Steel particle: R is the steel particle radius and ρ_{steel} is the mean SS316-steel density. The water volume unit is indicated with V_u.

green) is shaped as a rhomboid prism and the nucleus (in blue) as a cylinder, are modelled as water equivalent. The dimensions of each compartment are reported in Table 1 (right column). The water volume V_u, containing exactly a single cell and a tritiated steel particle deposited on the upper surface of the cell, represents our reference volume unit. Considering this ''single-cell single-particle'' configuration, the average dimension of a steel particle and the density of stainless steel (also presented in Table 1), one steel particle per volume unit V_u leads to a steel particle concentration of $1.33 \cdot 10^4$ μg/ml. Of note, this concentration is much higher than the particle concentrations in the cell culture medium used for experimental measurements published elsewhere (*13, 14*), which were in the range of 1–100 μg/ml. To make our computational approach applicable in realistic experimental conditions, a rescaling of simulation results to concentrations used for experiments is required, as discussed later.

TABLE 2
Experimental Information from the BEAS-2B Cell Culture Setup Used for Tritiated Particle Exposures and Radiobiological Measurements

Cells per well	40,000
Well surface	1.8 cm^2
Volume of medium in a well	800 μl
Confluency	60–70%
Steel particle concentration range	1–100 μg/ml
Specific activity	1 kBq/μg
Length of exposure	24 h

Note. Information is taken from data in references (*13, 14*) for a test of the computational approach for dosimetric reconstruction presented in this work.

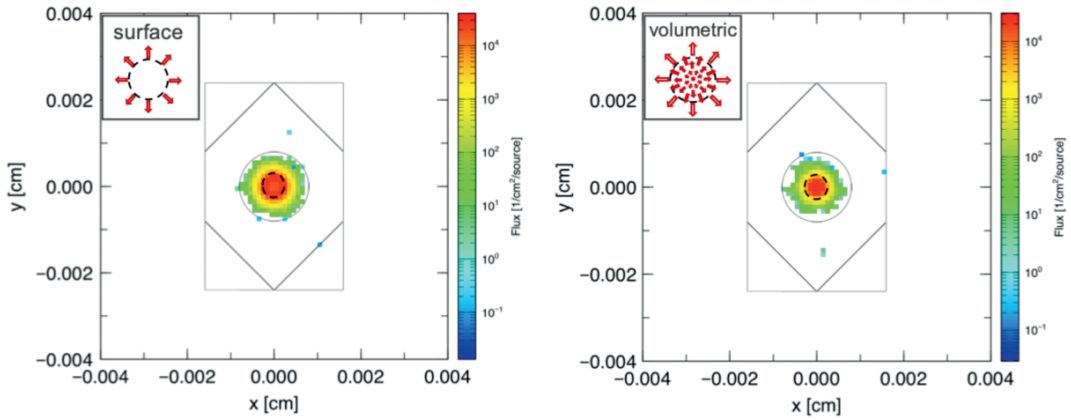

FIG. 2. Upper view of the single-cell single-particle software model with, in color for the flux scale, electrons emitted during tritium decays considering a surface source (left panel) or a homogeneous volumetric source (right panel).

Modelling Decays from the Tritiated Particles

Energy deposition to cell nuclei after tritium β-decays needs to be simulated within the model. Tritium decays into ^{3}He:

$$^3_1H \rightarrow {}^3_2He + e^- + \overline{\nu_e}.$$

The full energy distribution of emitted electrons was considered in the PHITS simulation. Tritium electrons have an average energy of 5.7 keV, corresponding to a range in water/tissue of ~0.5 μm, which is much smaller than the nuclear diameter, and a maximal energy of 18.6 keV, corresponding to a range in water/tissue of ~7.0 μm. As discussed later, the very short electron range corresponding to the average energy makes the positioning of the particle relative to the nucleus a key piece of information to perform a dosimetric assessment. In the present case, the tritium source is the tritiated steel particle. In the process of tritiation to produce radioactive particles for experimental measurements [see (*13, 14*)], tritium can be deposited only on the particle surface or could permeate beneath the surface, possibly being distributed in the whole particle volume. This information is not easy to access experimentally, and, due to the limited range of tritium decay electrons, it has an important impact on the chance that electrons reach the cell nucleus (*20*). In the simulations, we have therefore considered the two following kinds of tritiated particle sources: a ''surface source'', where tritium is only on the particle surface, and a ''volumetric source'', with tritium in the whole particle volume.

Predicting Radiation-Induced DNA Damage

Following the approach proposed by Kundrát et al. and Friedland et al. (*21, 22*), initial radiation-induced DNA damage yield can be quantified using analytical functions that reproduce damage as a function of the linear energy transfer (LET) of the radiation field in cell nuclei, the latter being estimated in its restricted form. Restricted LET in the cell nucleus as originally introduced in Kundrát et al. and Friedland et al. (*21, 22*) is conceptually equivalent to the dose mean lineal energy $\overline{y}_D$, i.e., the dose-average of the lineal energy y that can be interpreted as the microdosimetric equivalent for LET. Such analytical functions have been studied to reproduce full results of Monte Carlo calculations with PARTRAC (*5*, *16*), a biophysical code that simulates DNA damage induction starting from initial interactions of ionizing radiation (photons or different kinds of charged particles) in a water-equivalent cell model including a software replica of its genomic content. DNA damage is simulated both when induced directly (direct interactions of radiation with the DNA structure) or indirectly (energy deposition to water molecules surrounding the DNA, with formation and diffusion of radicals, that in turn can interact with DNA and damage it). Different kinds of DNA damage result from radiation action and can be predicted with the code. In particular, here we focus on sites with at least one DNA double-strand break, referred to as DSB sites, therefore including isolated DSBs and clusters of DSBs within a short genomic length (usually, less than 25 base pairs) that are still counted as a single DSB site. The $\overline{y}_D$-dependent yield of DSB sites is reproduced by:

$$Yield\ per\ cell\left[Gy^{-1}\right] = 6.6 \cdot \left(p1 + (p2\overline{y}_D)^{p3}\right) / \left(1 + (p4\overline{y}_D)^{p5}\right), \quad (1)$$

where $p1$-$p5$ are parameters depending on the type of radiation.

In our case, to apply this formula to predict DNA damage induction, we obtained the $\overline{y}_D$ quantity for a sensitive site of 1 μm diameter in the cell nucleus, due to tritium decay electrons. This is also possible with the code PHITS, that has a dedicated tally function to calculate the distribution of microdosimetric quantities in the scoring volume.

RESULTS

Dosimetric Estimates within the Single-Cell Single-Particle Software Model

We have performed dose calculations for both the surface and volumetric sources, since they represent the two extreme cases for a tritiated particle. Figure 2 shows a visual representation (in color scale for particle flux, for illustrative purposes) of electrons emitted from the particle for the surface (left panel) and volumetric (right panel) sources. To fully characterize the dose absorption by the cell nucleus, we performed different simulations varying the particle – nucleus center-to-center distance, referring to a two-dimensional geometry and considering an upper view of the cell. Therefore, we moved the steel particle on the upper surface of the cell, from the nucleus center along a radial axis with coordinate r (Fig. 3, left-side panel). For each configuration (particle–nucleus distance) we can calculate the S value, i.e., the absorbed dose to the target (cell nucleus) per decay from the source (steel particle) (Howell RW 1997). Results are presented in Fig. 3, for both the surface (blue curve) and volumetric (red curve) sources.

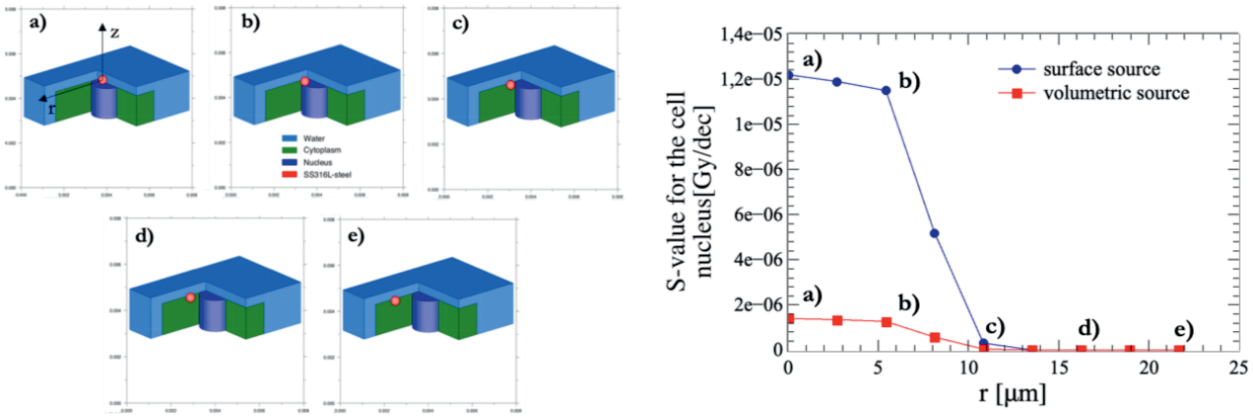

FIG. 3. Left panel: Different simulated configurations for the dose evaluation in the single-cell single-particle software model: the steel particle position changes along the *r* direction, corresponding to different particle – nucleus distances [increasing distance from panels a) to e)]. Right panel: Simulated S value for the cell nucleus [Gy/dec] as a function of the steel particle - nucleus distance (*r* [μm]) for the case of a surface source (blue line) and of a volumetric source (red line). Labels a)–e) refer to the geometrical configurations shown in the left panel.

The dose per decay to the nucleus is at a maximum when the particle lies over the nucleus, and it rapidly decreases when it is moved away. In particular, for both kinds of sources, the S value goes approximately to zero when the particle–nucleus distance is greater than ~11 μm. Given the average cell dimensions, this means that only one nucleus at a time can be reached from electrons emitted by a single tritiated particle. Using results shown in Fig. 3 in the range $0 < r < 11$ μm, we can calculate average S values for the surface and volumetric tritiated particle sources, which are 8.2 10^{-6} Gy/dec and 9.27 10^{-7} Gy/dec, respectively. The dose per decay to the nucleus is about one order of magnitude lower for the case of a volumetric source (both comparing average values, and the highest S values for particles closest to the nucleus). This is because electrons emitted from the inner volume of the steel particle lose part of their energy or are stopped already inside the particle itself, before reaching the nucleus.

It should be noted that the dose is still not homogeneously distributed inside the nucleus, since the range of electrons is much shorter than the nuclear dimensions and the electrons are thus stopped in the upper part of the nucleus. ''Local-doses'' to regions of cell nuclei in closer proximity to tritiated particles are expected to be higher, and this could have consequences on the spatial distributions of DNA damage, as discussed later.

To further investigate the potential impact of tritium associated with particle by-products, the dosimetric estimate was performed for a tritiated water (HTO) scenario. The simulation has been therefore repeated considering the whole volume V_u as source for tritium decays (hence the reference volume unit filled with tritiated water). The underlying assumption is that, due to water exchange between the cell and the environment, the whole cell volume is also available for the transport and decay of HTO molecules. The S value for the nucleus in this case (simply referred to as HTO in the following) is 1.16 10^{-5} Gy/dec. This value is dependent on the chosen volume unit V_u: the bigger the volume surrounding the nucleus, the lower the S value. It should not be used for a direct comparison to the S value for the tritiated particle source, but it is later used in the dosimetric reconstruction when the computational approach is applied to experimental cases.

From the Software Model to Experimental Conditions for In Vitro Cell Population Exposures

In the single-cell single-particle software model, we considered the presence of a steel particle on the cell surface in the volume unit V_u, which means a steel-particle concentration $C_{mod} = 1.33 \cdot 10^4$ μg/ml. This value is much higher than concentrations used for experimental measurements in (*13, 14*) (calculated as steel mass in the whole culture medium), which are in the range: $1 \leqq C_{exp} \leqq 100$ μg/ml. In real experimental conditions, steel particles settle at the bottom of the well, due to their high density, and deposit on the cell surface. The fraction of cells coming in contact with steel particles (and therefore, directly receiving dose from the particle, referred to as cells being ''hit'') clearly depends on the particle concentration in the medium: it is expected that not all cells will be hit by a particle for low concentrations. A method to go from our single-cell single-particle software model to realistic experimental conditions for in vitro exposures is therefore needed. We propose in what follows a general method, presenting its application to experimental conditions specified in Table 2 and adopted for measurements presented in (*13, 14*). In the published data (*13, 14*), cells were exposed to tritiated particles for 24 h. The main information that must be extracted from the simulations is therefore the cumulative dose to the cell nuclei population over the 24-h time interval. It also must be considered that, in real experimental conditions, part of the tritium carried by steel particles can be released into the cell culture medium. Due to the medium

TABLE 3
Results of the Computational Approach for Dosimetric Reconstruction on the Percentages of Cell Nuclei Receiving Dose from Tritiated Steel Particles

C_{exp} [μg/ml]	M/N_{nucl} [%]
1	0.4
50	20.1
100	40.1

Note. [M/N_{nucl} from Eq. (6)], for the three experimental concentration values Cexp (*13, 14*).

TABLE 4
Results of the Computational Approach for Dosimetric Reconstruction: Cumulative Dose to a Cell Nucleus in the Single Cell Single-Particle Model, for a 24 h Exposure to a Tritiated Steel Particle of Average Size

Source	d_{low} [Gy]	<d> [Gy]	d_{up} [Gy]
Surface	0.011	0.30	0.44
Volumetric	0.002	0.03	0.05

Note. [Eq. (5), in case of no-tritium release to the medium]: d_{low} and d_{up} are the dose lower and upper limits and <d> is the dose average value, obtained with the S values for a particle nucleus distance $r = 11$ μm, $r = 0$ μm and the average S value over the range $0 < r < 11$ μm, respectively.

composition, it can be assumed that released tritium is then distributed in the whole volume of medium in the form of HTO. The amount of tritium released necessarily affects the dosimetry. It is also expected that such a release process has a specific kinetics, meaning that the release might be continuously happening during the 24 h exposure period. Also, the particle deposition on the cell surface after administration to the cell culture is presumably time-dependent, starting at the beginning of the exposure. For the sake of simplicity, we made the following assumptions, later discussed in the light of the experimental data presented elsewhere (*13, 14*): 1. steel particles immediately deposit on the cell surface at the beginning of the exposure; 2. tritium release in the form of HTO is immediate and saturates at a given fraction of the total activity of tritiated particles.

The dosimetric reconstruction strategy then proceeds as follows: at a first stage, the dose calculations for realistic particle concentrations have been performed assuming two extreme cases: no tritium release from the particles and a complete tritium release scenario (HTO). The real condition, i.e., a combination of these two scenarios, is finally considered. We report in the following section the dose evaluation for three different C_{exp} values used elsewhere (*13, 14*): 1, 50 and 100 μg/ml, thus including the lowest and highest limits and an intermediate value, and for a given specific activity of 1 kBq/μg for tritiated particles.

To estimate the dose absorbed by the cell nuclei population in 24 h resulting from the tritiated particles, starting from our cell model, we need to determine the dose absorbed by a single nucleus and the fraction of nuclei within the well that are actually hit by the particles. To calculate the latter quantity, we first translated the three concentrations of steel particles into numbers of particles per well. Multiplying C_{exp}[μg/ml] by the volume of medium in the well [μl] (Table 2), we obtained the total steel mass per well. To obtain the particle number (n_{part}) for each C_{exp}, the total steel mass per well was divided by the mass of a single particle (obtained from data in Table 1). Since steel particles deposit only on the cell upper surface, we can refer to a two-dimensional geometry and consider only an upper view of the well. Assuming the steel particles and the cells evenly distributed within the total well surface A_{well} (Table 2), the surface fraction $A_{\%}$ occupied by cells that receive dose from the n_{part} particles is given by:

$$A_{\%} = \frac{A_{eff}}{A_{well}} \tag{2}$$

where A_{eff} is an ''effective area''. This area corresponds to the total area within which nuclei can receive dose from particles, i.e.,:

$$A_{eff} = \pi r^2 \cdot n_{part} \tag{3}$$

where r can be set from data shown in Fig. 3: since a nucleus receives a significant dose only if the nucleus – particle distance (center to center) is less than 11 μm, we have assumed $r = 11$ μm to calculate the effective area. It follows that only M of the total N_{nucl} nuclei in the well receive dose, where:

$$M = \frac{A_{eff}}{A_{well}} \cdot N_{nucl} \tag{4}$$

Table 3 reports the percentages of irradiated nuclei M/N_{nucl} [%] for the three steel particle concentrations considered. Only a very small percentage of cell nuclei (0.4%) is in contact with a particle for the lowest 1 μg/ml concentration. The percentage rises linearly with the concentration up to a ~40% for the 100 μg/ml case.

The second important quantity we need to estimate is the cumulative dose d absorbed by a single cell nucleus in a certain time interval due to a single tritiated steel particle. Such dose can be calculated as:

$$d[Gy] = S - value \cdot A_{source} \cdot m_{steel} \cdot t_{exp}, \tag{5}$$

where A_{source} [dec/(s·g)] is the steel particle specific activity (Table 2), m_{steel} [g] is the mass of a steel particle (from Table 1) and t_{exp} [s] is the exposure length of 24 h in this case. Table 4 reports the lower and the upper limits of d, d_{low} and d_{up}, together with its average value $\langle d \rangle$, for the surface and volumetric sources, calculated using the S value for $r = 11$ μm, $r = 0$ μm and the average S value over the range $0 < r < 11$ μm, respectively. On average, if a particle lies at less than 11 μm from its center, a nucleus absorbs a cumulative dose over 24 h of 30 cGy or 3 cGy, considering a surface or a volumetric source respectively.

TABLE 5
Results of the Computational Approach for Dosimetric Reconstruction: Cumulative Dose to a Single Cell Nucleus after 24 h Exposure to Different Steel Particle Concentrations, Calculated Assuming Complete Tritium Release to the Medium (Full HTO Scenario)

C_{exp} [μg/ml]	d [Gy]
1	$7.23 \cdot 10^{-5}$
50	$3.61 \cdot 10^{-3}$
100	$7.23 \cdot 10^{-3}$

At this point, we can obtain the dose to the cell nuclei population D, i.e., a dose estimate averaging over both cell nuclei within the well receiving radiation from tritiated particles and unirradiated ones, at end of a 24 h exposure. D is obtained by combining the two pieces of information calculated above:

$$D[Gy] = d \cdot M/N_{nucl}. \quad (6)$$

The average dose to the cell nuclei population, $\langle D \rangle$ and the lower and upper limits, D_{low} and D_{up}, can be obtained using in Eq. (6) $\langle d \rangle$, d_{low} and d_{up}, respectively. The average dose in case of a surface particle source has a wide range, from a few mGy up to hundreds of mGy for the concentration range considered (1.2 mGy at 1 μg/ml to 120 mGy at 100 μg/ml). In case of a volumetric particle source, the average dose to the population is of one order of magnitude lower in the same concentration range. From Eqs. (2–6) the dose to the cell nuclei population, given a dose value to the single cell in contact with a tritiated particle, also scales linearly with the particle concentration.

An analogous approach has been adopted to calculate the dose absorbed by the cell nuclei population in 24 h assuming complete and immediate tritium release by the steel particles or, in other words, a full HTO scenario. In this case, the percentage $M/N_{nucl}[\%]$ of nuclei receiving dose is 100%, since tritium becomes present in the whole well medium, including cell volumes, and all nuclei are receiving the same dose. We need therefore to calculate only the dose to a single cell nucleus d, which, for HTO conditions, can be defined as the dose absorbed by a single nucleus in a certain time interval for a given amount of tritium released by the tritiated particles in the volume unit V_u. It is reasonable to assume that such amount depends on steel particle concentration, hence on steel particle numbers n_{part}, and, more specifically, is proportional to the number of particles n_{Vu} that could be found in the volume V_u, if particles were distributed homogeneously in the whole medium instead of depositing at the bottom of the well. The number n_{Vu} can be easily obtained multiplying the ratio of the volume unit V_u to the total medium volume in the well by the n_{part} numbers for the different steel particle concentrations. The dose to a single cell nucleus has then been calculated using Eq. (5), using the S value previously calculated for the HTO case in the volume unit, and assuming that the activity of the tritium released by the n_{Vu} particles is the same as the activity of n_{Vu} tritiated steel particles. The dose values for the three C_{exp} are listed in Table 5. As mentioned, in the HTO case the dose to the cell nuclei population coincides with the dose to a single cell nucleus D, and the dose distribution is homogeneous.

Dosimetric Estimates for Realistic In Vitro Experimental Conditions

Experimental tests were conducted in parallel with radiobiological measurements [see (*13, 14*)] to quantify the fraction of initial tritium activity that is released by particles in the cell culture medium as a function of time. Activity measurements were performed by means of liquid scintillation for mineralized samples (total activity) and for the supernatant after separation of the particulate fraction (tritium released). In Fig. 4, we observe that the fraction of released activity is ~60% already after ~2 h, and this value tends to be stable afterwards. This trend was confirmed by the non-linear regression with a sigmoidal function, also shown in the figure. This ''saturation'' value seemed not to vary a lot with particle concentration. Given that ~2 h is a short time interval with respect to the duration of a 24 h exposure, and that the available data did not demonstrate a specific dependence of the amount of tritium release on particle concentration, we assumed that an average percentage of 60% of the total activity is immediately released in the medium in form of HTO, as previously anticipated. For this reason, the dose to the nuclei population in realistic experimental conditions can be estimated as: 40% of the dose for the ''no tritium release'' scenario (values from Table 4, after multiplication by the percentages of nuclei hit by steel particles given in Table 3) and 60% of the dose for the full HTO scenario (values from Table 5). The average dose values for the realistic scenario (obtained considering $\langle d \rangle$ values for ''no tritium release''), and the upper and lower dose limits for the realistic scenario (calculated using d_{low} and d_{up} for ''no tritium release'', respectively), are given in Table 6. Doses to the population in the realistic conditions are still mostly determined by cells in contact with particles, though of diminished activity, as the contribution of dose from HTO remains small in comparison. As an example, in case of a surface source for the highest particle concentration of 100 μg/ml: the average dose is of ~ 5.2 cGy, out of which 4.8 cGy (40% of 12 cGy, in turn obtained weighting the single-cell dose of 30 cGy with the 40% fraction of hit cells) come from decays from particles reaching the cells, and 0.4 cGy only from decays from HTO due to tritium release by particles in the medium.

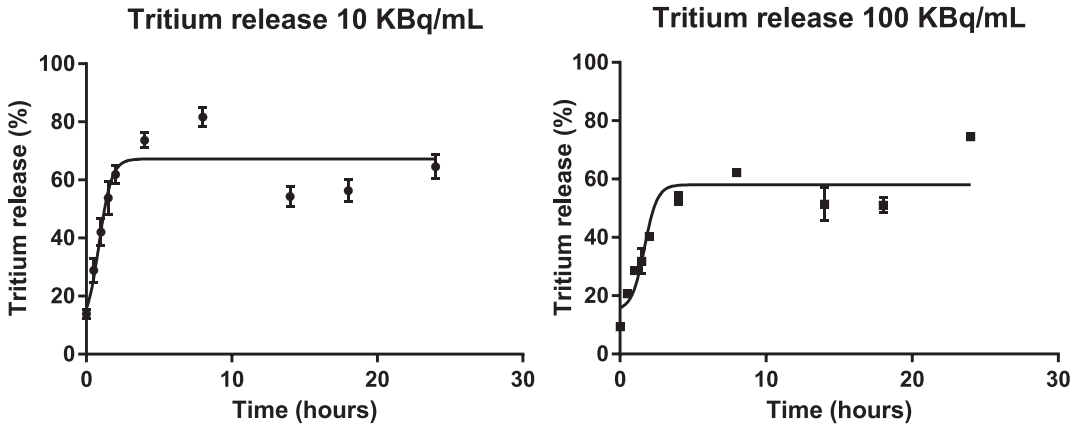

FIG. 4. Release of tritium activity in cell culture medium (percentage of total initial activity) as a function of time for two tested steel particle concentrations. The quantification of tritium activity has been performed by liquid scintillation counting for mineralized samples (total activity) and for the supernatant, after separation of the particulate fraction (tritium released). Data (Mean ± SEM, experiment in triplicates) are taken from (*13*). The fit is obtained with GraphPad Prism (GraphPad Prism s.d.) using non-linear regression with a three-parameter function: $Tritium\ release\ (\%) = B + (S - B)/(1 + exp(T_{50} - t))$, where B is a basal value (immediate release), S a saturation value and T_{50} is the time point at which the release is half-way between the basal and the maximal.

Impact on the Dosimetric Reconstruction of Particle Aggregates and Size Distribution

We can investigate the impact on the dosimetry related to the fact that more than one particle can deposit dose to the same cell at the same time. This can be due to the presence of particle aggregates, which has also been observed experimentally (*13, 14*), or simply to a non-homogenous distribution of particles in the well. For the highest concentration, a cell is hit on average by 0.4 particles (Table 3), which means that the probability of a cell being hit by two particles is not negligible according to a Poisson statistics. In such case, the ~ 6% of cells expected to be hit by two particles or, more generally, all cells hit by a particle aggregate would receive a different dose. We have therefore analyzed a scenario where two particles deposit onto the cell upper surface, and repeated the whole procedure described above. The dose to a single cell hit by two particles (considered as surface sources) positioned at its center is almost doubled (~40 cGy) when compared to the ~20 cGy in the single-cell single particle model (d_{up} value in Table 4 to be reduced by 40% to consider activity release from particle to the medium). This confirms that individual cells could receive doses higher than the upper limits discussed before, further increasing the dose heterogeneity in the cell population. However, for a fixed concentration (i.e., for a fixed number of particles per well n_{part}), if some cells are hit by more particles or particle aggregates, the fraction of hit cells M/N_{nucl} would remain lower, as other cells would become ''un-hit''. It is therefore expected that the average dose at the level of the cell population would always be of the same order of magnitude.

Similar considerations can be done if we want to quantify the impact on dosimetry of particles with different dimensions. In the calculations presented above we have considered steel particles with a single diameter, corresponding to the average value of the experimental particle size distribution [see ref. (*18*)]. Steel particles were found to have a fairly Gaussian size distribution with average radius $R = 2.35$ μm and $\sigma = 0.68$ μm (*13, 14*). We have therefore performed the dosimetric reconstruction using a combination of particles with three different radius values: R, $R + \sigma$ and $R - \sigma$, the abundance of each component being given by the corresponding weight in the Gaussian distribution.

TABLE 6
Results of the Computational Approach for Dosimetric Reconstruction: Cumulative Dose to the Cell Nuclei Population after 24 h Exposure in Realistic Experimental Conditions from Data found in Refs. (*13, 14*)

	Surface source			Volumetric source		
C_{exp} [μg/ml]	D_{low} [Gy]	<D> [Gy]	D_{up} [Gy]	D_{low} [Gy]	<D> [Gy]	D_{up} [Gy]
1	$6.15 \cdot 10^{-5}$	$5.23 \cdot 10^{-4}$	$7.54 \cdot 10^{-4}$	$4.59 \cdot 10^{-5}$	$9.75 \cdot 10^{-5}$	$1.25 \cdot 10^{-4}$
50	$3.08 \cdot 10^{-3}$	$2.61 \cdot 10^{-2}$	$3.77 \cdot 10^{-2}$	$2.30 \cdot 10^{-3}$	$4.88 \cdot 10^{-3}$	$6.24 \cdot 10^{-3}$
100	$5.15 \cdot 10^{-3}$	$5.23 \cdot 10^{-2}$	$7.54 \cdot 10^{-2}$	$4.59 \cdot 10^{-3}$	$9.75 \cdot 10^{-3}$	$1.25 \cdot 10^{-2}$

Notes. Experimental conditions are: 40% of tritium activity due to particles (''no-tritium release'') and 60% due to immediate tritium release to the medium forming HTO. The upper and lower dose limits are reported together with the average dose values, depending on cell particle, nucleus distance.

TABLE 7
Expected Cumulative Yield of Radiation-Induced DNA DSB Sites for a Single Cell Nucleus (Yield per Cell after 24 h) in Contact with a Tritiated Steel Particle in Realistic Experimental Conditions

	$Yield_{low}$ per cell	<Yield per cell>	$Yield_{up}$ per cell
DSB sites	0.5	7.1	10. 3

Notes. Average yield and lower and upper limits are given, considering the dose values for the surface source and the highest C_{exp} = 100 μg/ml case. Parameters used for DNA damage calculations in Eq. (1) taken from published article (Kundrát P 2020) are: p1 = 6.8; p2 = 0.1773; p3 = 0.9314; p4 and p5 are not applicable, i.e., terms not indicated by the track-structure simulations and hence not included in the given case. [Particle activity diminished to 40%, and 60% activity released to the medium (*13, 14*)].

As expected, the dose to a single cell nucleus hit by a tritiated steel particle significantly depends on the particle size. If a cell is hit by a particle of radius R + σ, the dose to the single cell nucleus can reach ~30 cGy for the surface source when the particle lies on top of the cell nucleus at its center. Such value is ~1.5 times higher than the corresponding value for a nucleus hit by a particle of average radius R (~20 cGy) and ~3 times higher than the corresponding value for a nucleus hit by a particle of radius R – σ (~9 cGy). However, the dose to the population associated to the particle size distribution does not vary significantly with respect to the case of all particles having average dimensions (differences are always below 10%), since the size distribution is symmetric, as well as the corresponding dose values. Again, the consideration of different particle sizes could lead to a further increase of the dose inhomogeneity, but average dose to the population at the same concentration would remain similar.

Prediction of Biological Effectiveness Based on Expected DNA Damage Induction

Some considerations can be made about the expected tritium-induced DNA damage in the simulated scenario, as an indicator of the biological effectiveness of tritiated steel particles of average size (only limited to the radiation-induced damage). To apply Eq. (1) to obtain the yield of DSB sites as a function the linear density of energy depositions by tritium radiation, we simulated with PHITS the dose distribution of the lineal energy $d(y)$ in a sensitive 1 μm diameter site in the cell nucleus, and obtained its first moment $\overline{y}_D$ in different exposure conditions. Simulation results indicate that $\overline{y}_D$ is mostly independent of the tritiated particle position with respect to the cell nucleus and of the kind of source (surface or volumetric particle sources or tritiated water) considered: as far as the cell nucleus is reached by tritium decay electrons, an almost constant $\overline{y}_D \sim$ 10 keV/μm is obtained for any of the considered scenarios. This value is reasonable considering that the average energy of 5.7 keV has a corresponding range of 0.5 μm. Considering such low $\overline{y}_D$ value, the yield for associated DNA damages was then calculated using in Eq. (1) the $p1 - p5$ parameters for protons (*22*) that are assumed to reproduce data for electrons and photons at the low-LET limits. Under the assumption of linearity of DNA damage yields with dose, we also obtained an estimate of the relative biological effectiveness (RBE) for tritiated particles: the RBE is given by the ratio of the damage yield following tritiated-particle exposure to the damage yield after external irradiation with an equal dose of a reference photon field. The dose mean lineal energy $\overline{y}_D$ for a reference photon field might vary in the range 2 to 4 keV/μm, depending on the field choice (e.g. ^{60}Co γ rays or kilo-voltage X rays). As Eq. (1) has an almost flat behavior for small $\overline{y}_D$. values, the damage associated to a reference photon field for RBE calculations, independent of the specific field choice, can be obtained when $\overline{y}_D \to 0$ in Eq. (1). Application of Eq. (1) leads to an expected yield of DSB sites of 57.1 per Gy per cell, when tritium electrons from a tritiated particle have reached the cell. This translates into a RBE value for this DNA damage endpoint of 1.3. This result indicates that the tritiated products we are considering are more effective than low-LET radiation such as photons, but their RBE is not much higher than 1.

It is then interesting to consider how these theoretical predictions translate into the possibility of empirical observation of DNA damage. Considering a single cell, the expected damage yield to the nucleus can be obtained by multiplying the yield of Eq. (1) by the dose to the nucleus as previously estimated.

When a cell is hit by a tritiated particle during the experiment, 40% of the particle activity is still effective in inducing damage directly to the cell, while 60% of tritium has been immediately released within the medium and has been integrated in HTO molecules distributed in the whole medium and cellular volumes. The DSB site yield associated with such exposure condition is therefore:

$$Yield\ per\ cell = \left[\left(40\% \cdot d_{part}[Gy]\right) + \left(60\% \cdot d_{HTO}[Gy]\right)\right] \cdot Yield\left[Gy^{-1}\right]. \quad (7)$$

Table 7 shows the average value of the expected yield for DSB sites and its lower and upper limits, obtained using in Eq. (8) as d_{part} the dose values due directly to the tritiated particle as a surface source (Table 4) and as d_{HTO} the dose due to tritiated water molecules for $C_{exp} = 100$ μg/ml (Table 5), thus representing an estimate of the expected radiation-induced DNA damage per cell in the worst-case scenario.

On the other hand, if a cell is not in direct contact with a particle instead, it can only receive dose from HTO, due to the tritium release from particles in the whole medium. The damage yield for a ''non-hit'' cell can be calculated using the 60% of the dose values given in Table 5. The value of expected DSB sites associated with the highest particle concentration, $C_{exp} = 100$ μg/ml, is reported in Table 8.

TABLE 8
Expected Cumulative Yield of Radiation-Induced DNA DSB Sites for a Single Cell Nucleus (Yield per Cell after 24 h not in Contact with a Steel Particle in Realistic Experimental Conditions

	<Yield per cell>
DSB sites	0.248

Note. (Damage Induced by tritium decays from HTO only, at the 60% of the initial particle activity), considering the highest C_{exp} . 100 μg/ml case.

These results are interpreted as follows: after a 24 h exposure, for a steel particle concentration of 100 μg/ml, all cell nuclei within the well are expected to experience a DNA damage of 0.25 DSB sites/cell due to tritium release from the particles. On top of that, only ~40% of cell nuclei are found in close contact with a tritiated particle deposited on their surface (see Table 3), experiencing additional damage due to electron decays from the particle surface (in these estimates). The total expected DNA damage for these nuclei can vary from 0.5 to 10.3 DSB sites/cell, depending on the relative position of the particle with respect to the cell nucleus, with an average value of 7.1 DSB sites/cell.

DISCUSSION

We developed a software model and a computational approach to perform the dosimetric assessment in case of in vitro exposure to different concentrations of tritiated steel particles of micrometric size. The distribution of particles with respect to cell nuclei has been modelled to characterize the radiation field produced by tritium decays from the particles with the radiation transport code PHITS. Indications on the expected biological effects induced by tritium decays from the particles have been obtained based on DNA damage predictions with the code PARTRAC.

To test the approach with realistic experimental conditions, we reproduced the specific features of the in vitro setup used elsewhere (*13, 14*), where genotoxicity tests were performed on the human lung cell line (BEAS-2B), exposed for 24 h to tritiated steel particles with a specific activity of 1 kBq/μg and concentrations up to 100 μg/ml (also see Table 2 for reference experimental conditions). Since a full characterization of the result of the tritiation process for particles used for in vitro studies is not easy to access experimentally, two different kinds of tritiated particle sources have been considered in the simulations: a surface source, where tritium is only on the particle surface, and a volumetric source, with tritium distributed in the whole particle volume. We expect that the real scenario lies in between these two extreme cases, likely closer to the surface source case, with tritium not deeply permeating into steel particles. Additional assumptions were made for the sake of simplicity, in particular: particles immediately deposit at the bottom of the well used for cell-culturing when administered to cells; they are homogeneously distributed within the well surface; they immediately release a 60% of their activity into the medium, in the form of HTO, as indicated by dedicated experimental measurements [results included in this work, see Fig. 4, and also reported in (*13, 14*)]. The modelling approach allowed the assessment of the cumulative dose received on average by the whole cell nuclei population in 24 h: this dose, even considering the upper dose limit of the surface source scenario for the highest 100 μg/ml particle concentration, remains very low, of the order of a few cGy. However, cells are far from being homogeneously irradiated, and at least two dose ranges should be considered separately, depending on the single cell being in contact (hit) or not with a tritiated steel particle (*24*). If cells are not directly in contact with a particle, they receive dose only from tritium released from particles into the medium. The dose to the cell nucleus in this case is only a few mGy, even for the highest particle concentration considered (100 μg/ml). If cells are directly hit by a tritiated particle, the dose to the nucleus further varies significantly depending on the relative position between the nucleus and the particle. In this case, the dose to the cell nucleus can reach ~ 20 cGy for the surface source when the particle lies directly on top of the cell nucleus. The dose to individual nuclei also varies significantly if they are hit by more than one particle at a time (because of a non-homogeneous distribution of particles in the well or because of particle aggregates), or by particles of different sizes. This increases the dose inhomogeneity among cells, though always with similar average doses to the population.

It is worth pointing out that the tritium concentration plays an important role in the population response, since it determines the percentage of cells hit by a particle, hence the percentage of cells possibly receiving a significant dose. This percentage is only 0.4% for the lowest concentration considered (1 μg/ml), but it rises to 40% for 100 μg/ml.

Analogous considerations apply to the DNA damage yield estimates. Here, we have reported results for sites of double strand breaks predicted with analytical functions of damage yield vs. dose mean lineal energy, adapted to reproduce simulation results with the biophysical code PARTRAC. DSB sites are an example of DNA damage with important biological consequences, whose LET-dependent behavior also appears well correlated to radiobiological measurements of LET-dependent cell killing (*25–27*). When a cell is not hit by a tritiated steel particle, the expected yield of DSB sites due to HTO is very low: on average, only one out of 4 analyzed cells should experience a radiation-induced DSB. On the contrary, a cell hit by a steel particle of average dimensions and receiving a significant dose is expected to experience up to 10 DSBs (initial damage, without considering the onset of repair processes, as later discussed) during the 24 h exposure.

It is interesting to note that our dose estimates obtained assuming complete tritium release (Table 5), i.e., a full tritiated water scenario, are of the same order of magnitude

of the results presented by Baiocco et al. (*28*), where a computational dosimetry approach is applied to reconstruct the cumulative dose absorbed in 24 h by an in vitro 3D model of the human airway epithelium exposed to tritiated water. Despite the differences in the experimental setups considered for the dosimetric reconstruction, since the ranges of tritium source activity and the exposure length analyzed in our work and in the work of others (*28*) are similar, as a first approximation the comparison of dose estimates in the two cases can be considered indicative.

The modeling strategy presented in this work is meant to be general and it can be used for a broad range of cases. Further refinements to the model, also depending on the experimental setup it is applied to, and on the availability of data for benchmark, are possible. As demonstrated by our results, the permeation of tritium in steel particles during tritiation plays an important role in the dosimetric reconstruction. A finer reproduction of the tritium initial distribution in particles and its release mechanism (e.g., considering the fast exchange between the resident ~few nm water layer around particles and the medium) could also be studied, using available information and with dedicated experimental measurements (*29–31*). The complete kinetics of tritium release in the medium as measured experimentally could also be considered, but data considered for this work suggests that this would not have a huge impact on the dosimetric assessment, at least for long exposures.

With the same modelling strategy, other kinds of particles could be considered, including tritiated cement particles, also studied by others (*13, 14*), hence with different elemental composition and dimensions as input for radiation transport simulations. Experimental data on interactions with the biological medium in terms of tritium release and particle solubility would equally be needed, to consider the loss of activity to the medium.

Results on the computational dosimetric reconstruction presented in this work can be further analyzed and correlated to the outcome of biological measurements. Experimental data from the in vitro setup of the BEAS-2B non-tumorigenic lung epithelial cell line exposed to tritiated steel particles are available elsewhere (*13, 14*). However, establishing a direct link between tritium exposure (reconstructed doses) and damage at the sub-cellular level (genotoxicity markers) remains non-trivial. In the literature (*13, 14*), measurements have been repeated also for hydrogenated (non-tritiated) particles as a control condition, to evaluate the possible damage due to contamination of cells with steel particles only. Based on a qualitative comparison between the effects of tritiated and hydrogenated steel particles, the authors conclude that radiative damage seems to play a role, and this seems to be more relevant at higher particle concentrations. As far as this is possible, quantitative comparisons should be performed, trying to ''subtract'' the damage due steel particles from the damage due to tritiated particles, highlighting and quantifying tritium effects. Also, a direct benchmark of simulation results on DNA damage induction with radiobiological data from genotoxicity assays is challenging. In the literature (*13, 14*) results are presented for the alkaline version of the COMET assay (measuring mainly DNA single strand breaks and alkaline labile sites) and for the cytokinesis-block micronucleus assay, identifying chromosome breakage and chromosome loss. For a better possibility of correlation with DNA damage predictions, DNA damage markers that can be better related to the initial DSB damage, as well as to its spatial distribution, should be preferred. DNA repair foci are a good candidate, also considering shorter exposures (maybe at a higher particle concentration or activity to compensate for the lower cumulative dose). Due to the prolonged nature of the exposure, it must be kept in mind indeed that what is measured is the result of the interplay between continuous damage induction and activation of DNA repair mechanisms. In addition to these considerations, the computational dosimetric assessment presented in this work indicates that the exposure is far from being homogeneous, especially at the lowest particle concentrations, with very few cells out of the whole cell population being hit by a steel particle. The data presented in the literature (*13, 14*) always show DNA damage markers are presented as averaged over the whole cell population. This provides indicators of the overall genotoxicity in the tested conditions, but the analysis of the full data distribution should be preferred, trying to discriminate, if possible, different levels of exposure. We believe that these considerations can be helpful to guide future experiments dealing with in vitro effects of tritiated (and, more generally, radioactive) particles, opening to the possibility of a thorough correlation with computational dosimetry to inform a dose-effect relationship.

As a general consideration, it is worth stressing again how computational modelling plays a key role in the dosimetric assessment in the framework of radiobiological studies of internal exposure to radionuclides, both for radiation protection and medical applications, as a direct measurement of radiation dose at the cell level is not feasible. As an example, recent studies on in vitro treatments with ^{177}Lu-DOTATATE radionuclide therapy have pointed out how the accuracy of the model in reproducing the experimental setup and, in particular, the cellular shape is critical for a good estimate of the dose absorbed by the cell nucleus, which is essential in enabling a clinically effective treatment (*33*). As expected, the spatial distribution of radionuclides, and the congruency of radioactive sources with cellular targets (which is the goal of radionuclide therapy for cancer cells) is of great importance, even more when considering short range emitters (*34*), among which tritium is an extreme case.

Finally, though a thorough discussion of the RBE of different tritiated products [and the many factors it depends on, see e.g., the systematic review in (*35*)] is beyond the

scope of this work, it is interesting to comment on our results in terms of RBE predictions for radiation-induced DNA damage due to tritiated steel particles. The RBE estimate of ~1.3 for the DSB site endpoint directly derives from the characterization of the radiation field in cell nuclei due to tritiated particle presence with a dose mean lineal energy of 10 keV/μm (PHITS results), which seems independent of the particle position with respect to the cell and of the kind of sources (particle sources, surface or volumetric, or HTO). This lineal energy is further translated in DSB site induction by means of PARTRAC. This RBE seems coherent with results obtained from experimental studies and simulations with a full HTO scenario. As an example, a RBE of exactly 1.3 is obtained with a full microdosimetric approach by Chen (*36*) when adopting a sensitive site of ~10 nm dimensions, which roughly corresponds to a ~30 base-pair length in the DNA model used for DNA damage predictions, with DSB sites also being scored on a similar length (*37*). Roch-Lefèvre (*7*) shows the RBE of OBT for chromosome aberrations induction was instead evaluated to be significantly higher than 1 at cumulative tritium doses below 10 mGy. The dose-dependence of OBT-induced chromosome aberrations was found however to be different from the classical linear-quadratic dependence that can be reproduced by DNA damage simulations with PARTRAC. This suggests that specific features of these tritiated products should be considered, as a particular spatial distribution and/or their active involvement in cellular pathways. At least in principle, we would not expect a strong analogy between the case of OBT and the case of tritiated steel micro-particles: at difference with OBT, these latter are expected to be recognized as ''foreign material'' by the cell machinery. It is useful to recall that the RBE estimate presented here only refers to the DNA damage that tritiated steel particles are expected to induce because of their radioactive nature. In an experimental measurement, unless this damage can be disentangled from the possible damage induced by non-radioactive particles of the same nature, the RBE concept itself might become difficult to apply.

It also must be recalled that single cells hit by steel particles (or even, as above-discussed, particle aggregates) would suffer high DNA damage (depending on individual dose levels) with respect to those reached only by HTO. Even if such ''hit'' cells may be only a few, if harboring a first gene or chromosome mutation but still viable, their presence can play a role in the initiation of a complex and long carcinogenesis process. Also, based on experimental data published elsewhere (*13, 14*) on the exposure of lung epithelial BEAS-2B cells to micrometric stainless-steel particles, we did not consider internalization of particles. It is expected that cells able to internalize such particles (as alveolar macrophages in case of particle inhalation) would receive higher doses, and this deserves a dedicated dosimetric reconstruction and further investigation in terms of possible associated biological effects.

Beyond the focus on tritiated products (*2*), the work presented here concerns current topics of broad and priority interest at present in low-dose radiation research. When dealing with internal contamination, the consideration of a distinct chemical speciation represents a novelty item in tritium research. It would also apply to other radionuclides: the specific chemical form is indeed always crucial in determining the biokinetics of radionuclides, their resulting spatial distribution at the organ/tissue/cellular and sub-cellular level, as well as the possible release of radioactivity to the microenvironment due to chemical and biological processes (*3, 38, 39*). When interpreting results of in vitro experimental exposures to make the bridge to the possible outcome at the organism level, it must be considered that the dose after radionuclide intake might be highly inhomogeneous. This is a general feature of many low-dose exposure scenarios (both at the spatial and temporal level), from environmental to medical exposures. Mechanisms responsible for biological effects of inhomogeneous dose deposition are not fully characterized, and the assessment of health risks of an inhomogeneous dose distribution is challenging, as well as the quantification of the impact of this single feature (*39, 40*). Finally, the study of such mechanisms becomes even more complex when the possible radiation-induced damage sums up to a bio-chemical damage due to contamination with non-biological materials.

In this general context, computational approaches as the one presented in this work to reconstruct radiation dose after contamination with radioactive products at the cell population level, as well as dose ranges for individual cells, provide essential information to inform dose-effect relationships. It fosters advancements in low-dose radiation research, aiming at the improvement of radiation protection standards including scenarios of exposures to peculiar radioactive by-products.

ACKNOWLEDGMENTS

This project has received funding from the Euratom Research and Innovation Programme 2014–2018 under grant agreement no. 754586. The views and opinions expressed herein do not necessarily reflect those of the European Commission. We thank C. Matthews of the Imaging Facility (IBDM, Aix-Marseille University, UMR 7288, Marseille, France) for his help in the realization of the confocal microscopy experiments and for the data processing. The IBDM laboratory is a member of the FBI national infrastructure supported by the National Research Agency (ANR-10-INBS-04). We also thank Walter T. Shmayda for scientific advice on tritium interactions with stainless steel.

Received: February 9, 2022; accepted: October 24, 2022; published online: November 28, 2022

REFERENCES

1. Dallas L J, Bean T P, Turner A, Lyons B P, Jha A N. Exposure to tritiated water at an elevated temperature: Genotoxic and transcriptomic effects in marine mussels (M. galloprovincialis). J Env Radioact. 2016; 64:325-336.
2. Liger K, Grisolia C, Cristescu I, Moreno C, Malard V, Coombs D, et al. Overview of the TRANSAT (TRANSversal Actions for

Tritium) project. Fusion Engineering and Design. 2018; 72, p. 136:168.

3. UNSCEAR. Sources, effects and risks of ionizing radiation. Annex C - Biological effects of 10 selected internal emitters-Tritium. 2017. pp. Available from: https://www.unscear.org/docs/publications/2016/UNSCEAR_2016_Report.pdf.
4. ICRP. Occupational Intakes of Radionuclides: Part 2. s.l.: ICRP Publication 134, 2016. Ann. ICRP 45(3/4). Available from: https://www.icrp.org/publication.asp?id=ICRP%20Publication%20134.
5. Little MP, Wakeford R. Systematic review of epidemiological studies of exposure to tritium. J Radiol Prot. 2008; 28:9-32.
6. Guégen Y, Priest N D, Dublineau I, Bannister L, Benederitter M, Durand C et al. In Vivo Animal Studies Help Achieve International Consensus on Standards and Guidelines for Health Risk Estimates for Chronic Exposure to Low Levels of Tritium in Drinking Water. Environ Mol Mutagen. 2018; 59:586-594.
7. Roch-Lefèvre S, Grégoire E, Martin-Bodiot C, Flegal M, Fréneau A, Blimkie M et al. Cytogenetic damage analysis in mice chronically exposed to low-dose internal tritium beta-particle radiation. Oncotarget. 2018; 9:27397-27411.
8. Priest N D, Blimkie M S J, Wyatt H, Bugden M, Bannister L A, Gueguen Y, et al. Tritium (3 H) Retention In Mice: Administered As HTO, DTO or as 3 H-Labeled Amino-Acids. Health Physics. 2017; 112: 439-444.
9. Bannister L, Serran M, Bertrdand L, Klokov D, Wyatt H, Blimkie M, et al. Environmentally Relevant Chronic Low-Dose Tritium and Gamma Exposures do not Increase Somatic Intrachromosomal Recombination in pKZ1 Mouse Spleen. Radiat Res. 2016; 186:539-548.
10. Quan Y, Lin J, Deng B. The response of human mesenchymal stem cells to internal exposure to tritium β-rays. J Radiat Res. 2019; 60:476-482.
11. Quan Y, Zhou C, Deng B, Lin J. The low dose effects of human mammary epithelial cells induced by internal exposure to low radioactive tritiated water. Tox In Vitro. 2019; 61:104608.
12. Wang K Z, Sun L, Xiong K H, Chen W B, Wang Y Y, Bian H H, et al. Monitoring of Tritium Internal Exposure Doses of Heavy-Water Reactor Workers in Third Qinshan Nuclear Power Plant. Dose Response. 2019; 22:17.
13. Report on acute and long-term toxicities, epi/genotoxic studies and transepithelial transfer of untritiated and tritiated particles on in vitro human models. 2022. TRANSAT Deliverables 3.7. https://transat-h2020.eu/wp-content/uploads/2022/06/TRANSAT_D3.7_Report_on_acute_and_long_term_toxicities_on_in_vitro_human_models.pdf
14. Lamartiniere Y, Slomberg D, Payet M, Tassistro V, Mentana A, Baiocco G, et al. Cyto-genotoxicity of tritiated stainless steel and cement particles in human lung cell models. Int J Mol Sci. 2022; 23:10398. (This article belongs to the Special Issue The Impact of Environmental Toxicants on Genetic and Epigenetic Stability)
15. Sato T, Iwamoto Y, Hashimoto S, Ogawa T, Furuta T, Abe S, et al. Features of Particle and Heavy Ion Transport code System (PHITS) version 3.02. J Nucl Sci Technol. 2019; 55, 6, pp. 684-690.
16. Friedland W, Dingfelder M, Kundrát P, Jacob P. Track structures, DNA targets and radiation effects in the biophysical Monte Carlo simulation code PARTRAC. Mutat Res. 2011; 711:28-40.
17. FIJI software. [Online] https://imagej.net/software/fiji/#publication.
18. Report on production of steel particles. 2019. TRANSAT Deliverables D3.1. http://transath2020. eu/.
19. Report on production of cement particles and characterization on steel and cement suspension. 2019. TRANSAT Deliverables D3.2. http://transat-h2020.eu/.
20. Torikai Y, Penzhorn R-D, Matsuyama M, Watanabe K. Chronic Release of Tritium from SS316 at Ambient Temperature: Correlation Between Depth Profile and Tritium Liberation. Fusion Science and Technology. 2005; 48, p. 177.
21. Friedland W, Schmitt E, Dingfelder M, Baiocco G, Barbieri S, Ottolenghi A. Comprehensive track-structure based evaluation of DNA damage by light ions from radiotherapy relevant energies down to stopping. Sci Rep. 2017; 7, 45161.
22. Kundrát P, Friedland W, Becjer J, Eidemüller M, Ottolenghi A, Baiocco G. Analytical formulas representing track-structure simulations on DNA damage induced by protons and light ions at radiotherapy-relevant energies. Sci Rep. 2020; 10, 15775.
23. Howell RW, Dandamudi WR, Bouchet L, Bloch W, Goddu SM. MIRD Cellular S Values. https://www.snmmi.org/Store/ProductDetail.aspx?ItemNumber=8862
24. Emerging Issues on Tritium and Low Energy Beta Emitters. T, Goodhead D. [ed.] European Commision Series. Luxembourg: Radiation Protection 152, 13 November 2007.
25. Davidkova M, Kundrat P, Stepan V, Palajova Z, Judas L. Lethal events in V79 cells irradiated by low-energy protons and correlations with distribution patterns of energy deposition, radical concentratiom and DNA damage. Appl. Radiat. Isot. 2009; 67:454-459.
26. Friedland W, Jacob P, Paretzke H G, Ottolenghi A, Ballarini F, Liotta M. Simulation of light ion induced DNA damage patterns. Rad. Prot. Dosim. 2006; 122:116-120.
27. D, Kundrát P, Stewart R. On the biophysical interpretation of lethal DNA lesions induced by ionising radiation. Rad. Prot. Dosim. 2006; 122:169-172.
28. Baiocco G, George I, Garcia-Argote S, Guardamagna I, Lonati L, Lamartinière Y, et al. A 3D in vitro model of the human airway epithelium exposed to tritiated water: Dosimetric estimate and cytotoxic effects. Radiat Res. 2021; 195:265-274.
29. Sharpe M, Fagan C, Shayda W T. Distribution of Tritium in the Near Surface of Type 316 Stainless Steel. Fusion Sci Tech. 2019; 75:1053-1057.
30. Sharpe M D, Fagan C, Shayda W T, Shröder W U. Partitioning of tritium between surface and bulk of 316 stainless steel at room temperature. Fusion Eng Design. 2018; 130:76-79.
31. Sharpe M, Shmayda W T, Shröder W U. Tritium Migration to the Surfaces of Type 316 Stainless Steel; Aluminum 6061; and Oxygen-Free, High-Conductivity Copper. Fusion Sci Tech. 2016; 70:97-111.
32. Quinlan M J, Shmayda W T, Lim S, Salnikov S, Chambers Z, Pollock E, et al. Effects of H2O and H2O2 on Thermal Desorption of Tritium from Stainless Steel. Fusion Sci Tech. 2008; 54:519-522.
33. Tamborino G, De Saint-Hubert M, Struelens L, Seoane D C, Ruigrok E A M, Aerts A, et al. Cellular dosimetry of [177Lu]Lu-DOTA-[Tyr3]octreotate radionuclide therapy: the impact of modeling assumptions on the correlation with in vitro cytotoxicity. EJNMMI. 2020; 7:8.
34. Siragusa M, Baiocco G, Fredericia P M, Friedland W, Groesser T, Ottolenghi A, et al. The COOLER Code: A Novel Analytical Approach to Calculate Subcellular Energy Deposition by Internal Electron Emitters. Radiat Res. 2017; 188, pp. 204-220.
35. Little MP, Lambert BE. Systematic review of experimental studies on the relative biological effectiveness of tritium. Radiat Environ Biophys. 2008; 47:71-93.
36. Chen J. Radiation quality of tritium: a comparison with 60Co gamma rays. Radiat Prot Dosim. 2013; 156:372-5.
37. Goodhead DT. Energy deposition stochastics and track structure: what about the target? Radiat Prot Dosim. 2006; 122:3.15.
38. Vorob'eva NY, Kochetkov OA, Pustovalova MV, Grekhova AK, Blokhina TM, Yashkina EI, et al. Comparative Analysis of the Formation of gammaH2AX Foci in Human Mesenchymal 7 Stem Cells Exposed to (3)H-Thymidine, Tritium Oxide, and X-Rays Irradiation. Bull Exp Biol Med. 2018; 166:178-81.
39. Strategic Research Agenda of the Multidisciplinary European Low Dose Initiative. 2021. MELODI. https://melodi-online.eu/news/

2021-strategic-research-agenda-sra-and-sra-statement-now-available/.

40. Baiocco G, Bartzsch S, Conte V, Friedrich T, Jackob B, Tartas A et al. A matter of space: how the spatial heterogeneity in energy deposition determines the biological outcome of radiation exposure. Radiat Environ Biophys. 2022; 61:545-559.

41. GraphPad Prism. [Online] https://www.graphpad.com/scientific-software/prism/.